Simultaneous single-molecule measurements of phage T7 replisome composition and function reveal the mechanism of polymerase exchange

Joseph J. Loparo, Arkadiusz W. Kulczyk, Charles C. Richardson[1], and Antoine M. van Oijen[1,2]

Department of Biological Chemistry and Molecular Pharmacology, Harvard Medical School, Boston, MA 02115

Contributed by Charles C. Richardson, December 17, 2010 (sent for review September 29, 2010)

A complete understanding of the molecular mechanisms underlying the functioning of large, multiprotein complexes requires experimental tools capable of simultaneously visualizing molecular architecture and enzymatic activity in real time. We developed a novel single-molecule assay that combines the flow-stretching of individual DNA molecules to measure the activity of the DNA-replication machinery with the visualization of fluorescently labeled DNA polymerases at the replication fork. By correlating polymerase stoichiometry with DNA synthesis of T7 bacteriophage replisomes, we are able to quantitatively describe the mechanism of polymerase exchange. We find that even at relatively modest polymerase concentration (~2 nM), soluble polymerases are recruited to an actively synthesizing replisome, dramatically increasing local polymerase concentration. These excess polymerases remain passively associated with the replisome through electrostatic interactions with the T7 helicase for ~50 s until a stochastic and transient dissociation of the synthesizing polymerase from the primer-template allows for a polymerase exchange event to occur.

bacteriophage T7 | DNA replication | flow stretching | fluorescence

The replisome, a multiprotein complex that carries out DNA replication, is thought of as a stable molecular machine that duplicates genomic DNA in a rapid and continuous fashion (1). Even though high processivities and rates are observed in vitro (2), replisomes in a cellular environment face numerous obstacles including transcription complexes and DNA lesions that may stall the replicative polymerase (3). Recent work has challenged the notion that a single, unchanging replisome is able to replicate a complete genome in vivo (4, 5). The discovery of translesion DNA polymerases, specialized enzymes capable of synthesizing across damaged DNA bases, and novel mechanisms for replication restart suggest that the replisome might be highly dynamic, with components exchanging and entire replisomes collapsing and reassembling (6).

Biochemical experiments have provided, at least at first glance, contradictory information regarding the stability of a key component of the replisome, DNA polymerases. Textbook models have portrayed the leading-strand polymerase as remaining tightly associated with the replisome, synthesizing DNA in a continuous fashion. On the lagging strand, the regular and rapid completion of Okazaki fragments requires either the recycling of the lagging-strand polymerase to the new RNA primer or the recruitment of a new polymerase from solution. Experiments have revealed that the replisomes of *Escherichia coli*, as well as the T4 and T7 bacteriophages remain highly processive even when challenged by dilution (7–10). At the same time, however, the T4 and T7 leading- and lagging-strand DNA polymerases exchange rapidly when challenged with excess polymerase in solution (11, 12). Similar results have been obtained in *E. coli*, where translesion DNA polymerases are able to replace DNA polymerase III at both lesions and on undamaged DNA (13, 14). Benkovic and coworkers attempted to reconcile these seemingly contradictory dilution and challenge experiments by proposing that specific protein-protein interactions can serve to both confer processivity and mediate exchange of replisome components (11).

Ultimately, a dynamical description of these exchange and (dis)assembly processes requires experimental techniques that can detect the essential intermediates and observe their appearance and disappearance in real time. Motivated by this necessity, we developed a unique single-molecule assay capable of correlating the activity of individual replisomes with their composition and stoichiometry in real time. We describe the development of this assay and how we have applied it to determine the mechanism by which polymerases exchange in the bacteriophage T7 replisome.

The bacteriophage T7 replisome is an ideal model system for studying replication dynamics because it recapitulates the key features of more complicated systems, yet can be reconstituted in vitro with only four proteins. DNA synthesis is carried out by a stable, one-to-one complex of gene 5 protein (gp5) and thioredoxin, a processivity factor produced by the *E. coli* host. Gene 4 protein (gp4) contains both helicase and primase domains whereas gene 2.5 protein (gp2.5) is the single-stranded DNA binding protein (15).

A previous report by one of our laboratories found that the T7 replisome, which is processive in the absence of excess polymerase in solution, undergoes leading- and lagging-strand polymerase exchange when challenged with a 10-fold excess of polymerase (12). This exchange required gp4, suggesting that specific protein-protein interactions between the helicase and polymerase mediate this process. Subsequent work by our laboratories examined the interaction between the polymerase and helicase using surface plasmon resonance and found that in the absence of DNA synthesis a polymerase was able to associate with a C-terminal tail of gp4 monomers through electrostatic interactions in a DNA-independent fashion (16). Single-molecule experiments indicated that deletion of the gp4 C-terminal tail decreased the processivity of a polymerase preassembled on the leading strand, indicating that this interaction can capture synthesizing polymerases that transiently dissociate from the primer.

Here we directly visualize DNA polymerase exchange during leading-strand synthesis by correlating the arrival of fluorescently labeled polymerases at the fork with changes in DNA synthesis. Performing these experiments at the level of individual T7 replisomes allows us to quantify the kinetics of the polymerase exchange reaction, which were previously obscured in ensemble-

Author contributions: J.J.L., C.C.R., and A.M.v.O. designed research; J.J.L. and A.W.K. performed research; J.J.L. and A.W.K. analyzed data; and J.J.L., C.C.R., and A.M.v.O. wrote the paper.

The authors declare no conflict of interest.

See Commentary on page 3459.

[1]To whom correspondence may be addressed: E-mail: ccr@hms.harvard.edu or a.m.van.oijen@rug.nl.

[2]Present address: Zernike Institute for Advanced Materials, University of Groningen, Groningen 9747 AG, The Netherlands.

This article contains supporting information online at www.pnas.org/lookup/suppl/doi:10.1073/pnas.1018824108/-/DCSupplemental.

level experiments. We find that excess polymerases transiently associate with gp4 and subsequently "wait" for the synthesizing polymerase to stochastically dissociate from the primer before polymerase exchange can occur. The strength of the interaction between gp4 and an excess polymerase makes the frequency of exchanges sensitive to the concentration of soluble polymerase. This effect arises due to the concentration-dependent change in the average occupancy of polymerase bound to the hexameric helicase. Deletion of the presumptive interaction between gp4 and a polymerase from solution, accomplished by truncating the C-terminal tail of gp4, dramatically reduces the number of polymerase exchange events. These results indicate that the same interaction between helicase and polymerase that confers processivity to the replisome in the absence of excess polymerase also facilitates the exchange of DNA polymerases.

Results

Single-Molecule Experimental Design. Obtaining a molecular-level understanding of polymerase exchange on the ensemble level is difficult for two reasons: Exchange events occur stochastically, and intermediate states may be short-lived or nonaccumulating. Thus, single-molecule methods capable of visualizing individual replisomes are promising tools for observing replication-fork dynamics. A particularly powerful approach, which has been pursued with great interest, is to combine nanomanipulation methods, such as optical or magnetic tweezers, with fluorescence techniques to correlate structure and function at the single-molecule level (17). The few reported examples of this approach have been limited to measuring single DNA substrates at a time, which precludes the simultaneous examination of many molecular machines that is normally required to detect rare events (18–20).

Previously we described how the flow-stretching of tethered DNA can be used to simultaneously characterize the activity of hundreds of individual bacteriophage T7 and *E. coli* replisomes (21, 22). In these experiments, a laminar flow of buffer through a flow cell exerts a hydrodynamic drag force on a bead that is attached to the end of a surface-tethered λ phage DNA with replication fork and primer. Stretching forces of 2–4 pN cause double-stranded DNA to be extended to nearly its crystallographic contour length whereas ssDNA remains entropically collapsed on itself (23, 24). Therefore, catalytic activity of the replisome that converts dsDNA to ssDNA, or vice versa, is observed as a shortening/lengthening in the overall length of the DNA (25, 26).

To observe the composition of the replisome, we employed single-molecule fluorescence imaging to correlate fluorescence intensity with stiochiometry at the replication fork. We visualized the association of the T7 DNA polymerase with the replisome, by labeling its processivity factor thioredoxin with Alexa-fluor 555 dye (see *Methods*). Mixing the labeled thioredoxin with T7 gp5 yields a processive DNA polymerase whose activity in a bulk leading-strand synthesis assay is identical to the wild-type protein (*SI Text*).

To combine the flow stretching of DNA with the imaging of fluorescently labeled proteins, we employed total-internal reflection fluorescence (TIRF) microscopy to reduce the background contribution from proteins not associated with the replisome (27). The micron-scale beads we had used previously to stretch and image the length of DNA are not compatible with TIRF microscopy due to their size and brightness as compared to single fluorophores. As an alternative, we labeled DNA with quantum dots (QDs). End labeling of the DNA with QDs results in poor spatial resolution of the DNA length due to the negligibly small Stokes drag force on the QD and, as a result, significant Brownian fluctuations of the QD (see Fig. 1*A*). Site-specifically labeling the DNA with a QD (28, 29) at ~15 kilobases (kb) from the surface-tethered replication fork results in dramatically improved results

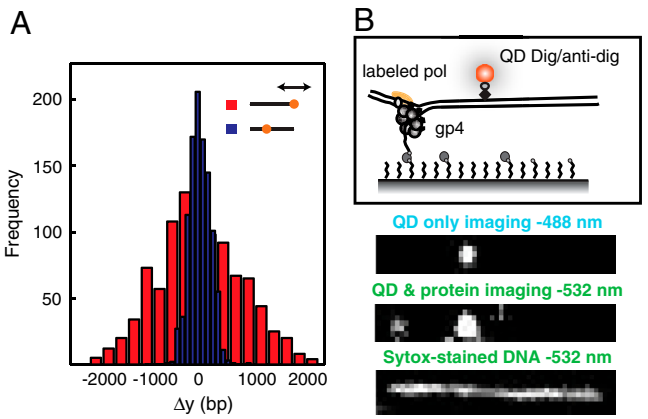

Fig. 1. Single-molecule assay to measure replisome composition and activity. (*A*) The length of flow-stretched DNA is monitored by tracking the position of a quantum dot attached to the DNA. The longitudinal (i.e., in the direction of flow) position fluctuations are shown for a DNA labeled with a QD at the end of the 48-kb long DNA (red) and for one labeled 14.8 kb downstream from the anchor point (blue). (*B*) Two-color imaging scheme used to continuously track QD position while stroboscopically observing fluorescently labeled T7 DNA polymerases. A DNA construct with replication fork and site-specifically labeled with a QD is attached to the surface of a flow cell through a biotin-streptavidin linker. Evanescent excitation illuminates the bottom surface of the flow cell, allowing one to selectively observe QDs with 488 nm excitation and image both labeled proteins and QDs with 532 nm light.

due to the ~30 kb of dsDNA after the tethered QD that acts as a "molecular sail" to stretch the DNA. Wide-field TIRF imaging allows us to observe many DNA substrates at a given time; typical fields of view under 60× magnification contain 50–100 DNA-tethered QDs.

The replication reactions we wished to observe occur stochastically over an approximately 10 min window, much longer than the typical photobleaching lifetime of a protein labeled with an organic fluorophore. Imaging with 488 nm excitation allowed for selective and continuous imaging of the QD (see Fig. 1*B*). Given the large disparity in extinction coefficients between the QD and the dye at 488 nm (1,100,000 to 10,000) the dye is not significantly excited by the QD imaging, preventing its rapid photobleaching. Stroboscopic imaging of the labeled polymerase and QD was accomplished by using 532 nm laser excitation every 7 s, which greatly extended the observation window of the polymerase (*SI Text*).

Excess Polymerase in Solution Associates with the T7 Replisome. To observe the exchange of leading-strand polymerases, we preassembled an unlabeled T7 DNA polymerase and gp4 helicase/primase onto DNA in the absence of Mg^{2+} ions, washed the flow cell extensively to ensure no polymerase was present in solution and then initiated DNA synthesis via injection of a buffer containing Mg^{2+}, deoxyribonucleotide triphosphates (dNTPs), and labeled T7 polymerase. In the absence of lagging-strand DNA synthesis, gp4 and the leading-strand polymerase convert the lagging-strand template into ssDNA, resulting in a shortening of the DNA construct (21) (see Fig. 2*A*). As anticipated, DNA synthesis began without a labeled polymerase at the replication fork (Fig. 2*B*). In approximately 20% of these events, a labeled polymerase appeared at the fork prior to the cessation of DNA synthesis. Several examples of such events are shown in Fig. 2*B*. The appearance of the labeled polymerase at the replication fork did not alter or pause leading-strand synthesis.

We found that the intensity of polymerase fluorescence varied with time, suggesting changes in polymerase stoichiometry at the replication fork. Integrating over a 3×3 pixel box centered at the forked DNA-tether point showed rather discrete changes in the level of fluorescence, consistent with the arrival and depar-

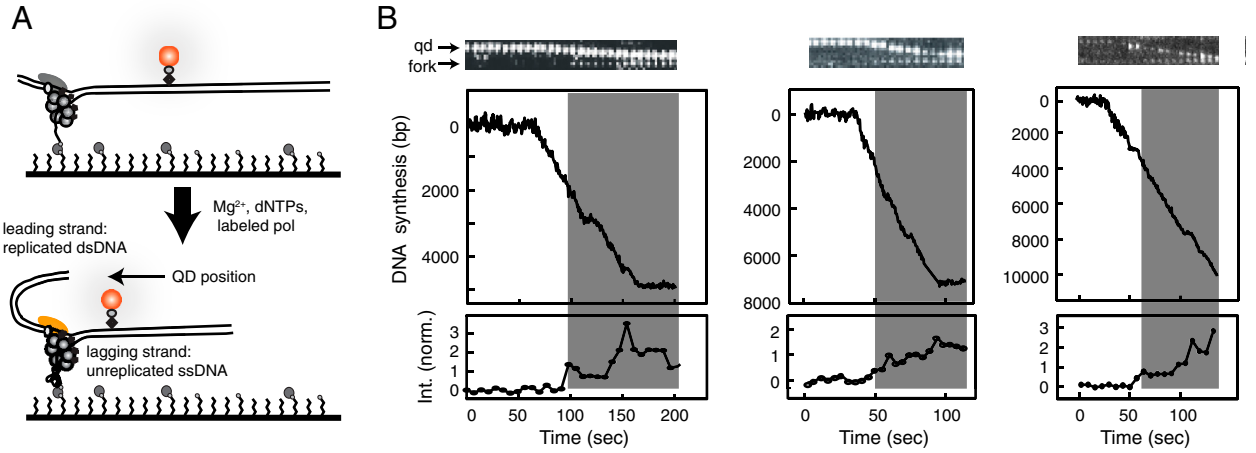

Fig. 2. Leading-strand DNA synthesis and the association of labeled DNA polymerase with the replication fork. (*A*) Cartoon depicting the experimental approach. An unlabeled, leading-strand DNA polymerase and helicase are preassembled on DNA and excess proteins are washed out. DNA synthesis is initiated by flowing a buffer containing Mg^{2+} ions, dNTPs, and excess fluorescently labeled DNA polymerase. DNA synthesis is observed as a shortening of the length of DNA as monitored by tracking the position of the QD. Lagging-strand synthesis does not occur because the ribonucleotides necessary for the priming of Okazaki fragments are excluded. (*B*) Example trajectories showing the appearance of a labeled polymerase at the replication fork during DNA replication. The top panels are kymographs constructed from images taken every 7 s. The QD is seen moving against the flow of buffer, indicating leading-strand synthesis, whereas the labeled polymerase, initially absent, associates with the replisome. The middle panels show the QD trajectory whereas the bottom panels depict the integrated intensity at the replication fork as a function of time.

ture of individual polymerases (Fig. 2*B*, *Lower*). The arrival of multiple polymerases at the fork suggests an interaction with gp4, a hexamer with six equivalent binding sites. Polymerases remained associated with the replisome for tens of seconds, much longer than one would anticipate for nonspecific binding to ss- or dsDNA (30). Collectively these results indicate that polymerases from solution are capable of associating with an active replisome presumably through interactions with gp4 monomers.

A Polymerase Mutant Allows for the Characterization of Exchange Kinetics. In the above experiments, the preassembled, unlabeled, and competing, labeled polymerases were catalytically identical. We therefore could not determine when exchange of the active polymerase occurred. To address this issue, we employed an unlabeled polymerase mutant, Y526F. Replacement of tyrosine at position 526 with phenylalanine in the nucleotide binding pocket slows the average rate of DNA synthesis of the polymerase (12, 31). We observed a 2.5-fold difference (122 ± 5 bp/s to 48 ± 2 bp/s) that was readily detected at the single-molecule level (Fig. 3 *A* and *B*). Strikingly, DNA replication reactions containing a 1:1 mix of both polymerases (green line, Fig. 3*A*) exhibited trajectories characterized by numerous abrupt changes in the rate of synthesis. This observation is consistent with exchange of the synthesizing polymerase and provides a means to monitor when exchanges occurred in real time.

Mechanistic insight into the polymerase exchange reaction was gained by correlating changes in the DNA synthesis rate with the fluorescence from labeled WT polymerases at the replication fork. Replication reactions were run by flowing a 1:1 mix of labeled WT polymerase and unlabeled Y526F polymerase with gp4 and dNTPs through a flow cell containing tethered DNA. Synthesis events by unlabeled Y526F DNA polymerase that include the transient appearance of labeled WT polymerase at the fork and its subsequent disappearance with no increase in the rate of DNA synthesis, report directly on the strength of the presumptive interaction between an excess polymerase and gp4. Examples of such trajectories are shown in Fig. 3*C*. Here, the length of time in which the labeled polymerase remains bound to gp4, τ_{off}, reports directly on the off rate or dissociation rate of the protein–protein complex. On average a labeled polymerase remained bound to gp4 for 44 ± 6 s (mean $\pm$ SEM), see Fig. 3*D*. We were unable to measure the on rate directly as there is no well-defined time zero for when the labeled polymerase reaches the surface of the flow cell.

Under the same experimental conditions we observed events that began with Y526F synthesis followed by the association and subsequent exchange of a labeled WT polymerase, as shown in Fig. 3*E*. These events report on the time elapsed between polymerase association and exchange, τ_{exc}. Our results indicate that polymerase exchange was not immediate; instead the polymerase from solution remains passively associated with gp4 until presumably the synthesizing polymerase disengages from the primer template. On average this delay time between association and exchange, τ_{exc}, is 55 ± 15 s. The consequent change in the rate of synthesis is often abrupt, indicating that the actual process of switching polymerases at the fork is rapid. Together these results demonstrate that by mixing labeled WT and unlabeled Y526F polymerase we are able to identify and quantify the kinetic steps of the polymerase exchange reaction.

Exchange Kinetics Depend Sensitively on the Concentration of Excess Polymerase. Observing events that begin with Y526F synthesis and show exchange to the WT were rare (<10% of observed synthesis events) as the concentration of the labeled polymerase was kept low enough ($< \sim 1$ nM) to keep the fluorescent background from overwhelming the signal from individual labeled proteins. To further quantify the exchange kinetics, we examined the rate of exchange in the presence of increasing concentrations of the Y526F DNA polymerase. An unlabeled WT leading-strand polymerase and gp4 were preassembled on a replication fork, free protein was washed out, and synthesis was initiated in the presence of different concentrations of unlabeled Y526F. In the absence of Y526F polymerase, the average processivity of a WT leading-strand event was 15.2 ± 3.4 kb, consistent with our previously reported value (21). Addition of Y526F resulted in a subset of trajectories that displayed initial synthesis at WT rates and then exhibited a change in rate consistent with exchange to Y526F (Fig. 4*A*). Increasing the concentration of Y526F resulted in a higher percentage of trajectories exhibiting exchange and a decrease in the average processivity of WT synthesis. Fig. 4*B* shows how the average WT processivity, calculated by including all events of DNA synthesis, changed as a function of the challenging Y526F concentration. At a Y526F concentration of

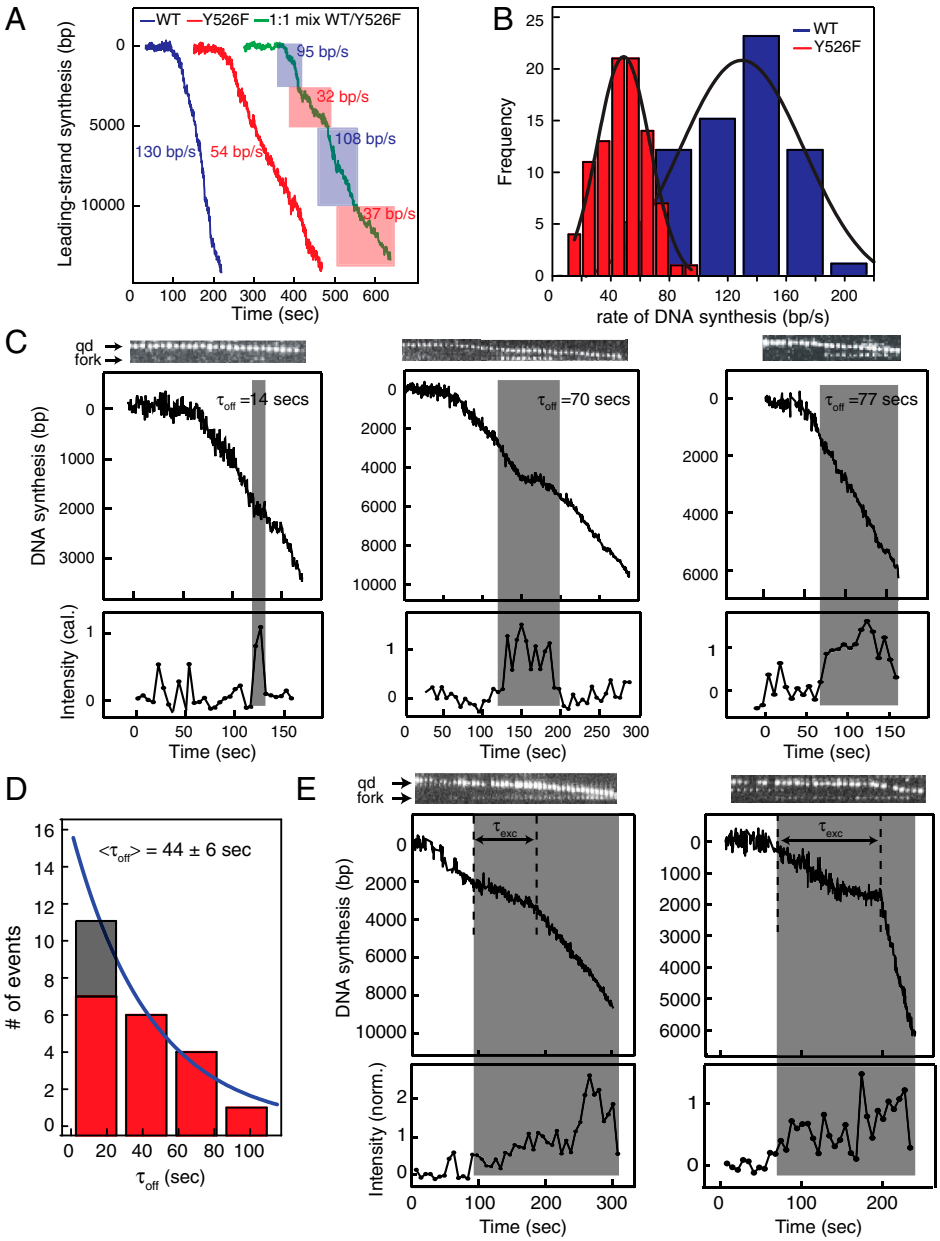

Fig. 3. Exchange of DNA polymerases at the replication fork. (*A*) WT T7 DNA polymerase and Y526F polymerase mutant have different rates of DNA synthesis. The panel shows example trajectories of leading-strand synthesis with WT polymerase only (blue line), Y526F polymerase mutant only (red line), and a 1:1 mix of WT and Y526F polymerase (green line). The abrupt changes in DNA synthesis in the green trajectory are due to exchange of the synthesizing DNA polymerases. (*B*) A histogram showing the distribution of rates of synthesis for WT (blue) and Y526F (red) polymerases. (*C*) Example trajectories showing the transient association and dissociation of a labeled polymerase without exchange. For each individual trajectory the top panel shows a kymograph of images taken every 7 s, the middle panel shows the leading-strand synthesis trajectory resulting from tracking the QD position and the bottom panel shows the fluorescent intensity at the replication fork. (*D*) A histogram showing the τ_{off} times taken from individual events of association and subsequent dissociation without polymerase exchange. The data are fit with an exponential decay not taking into account the undersampled first bin. (*E*) Example trajectories illustrating the association of a labeled polymerase with the replisome and subsequent polymerase exchange from unlabeled Y526F to labeled WT polymerase.

20 nM approximately 75% of the traces showed exchange with an average WT processivity of 3.3 ± 0.6 kb.

Polymerase Exchange Is Mediated Through Interactions with gp4. We previously determined that a preassembled leading-strand complex of WT polymerase with a helicase mutant lacking 17 residues of the C-terminal tail, gp4-ΔC17, exhibits an average processivity of only 5 ± 1 kb (16). From this data, it was proposed that the interaction between the polymerase and the C-terminal tail of gp4 act to confer processivity by tethering polymerases that transiently dissociate form the primer. These fleeting dissociations of the synthesizing polymerase are the putative pathway by which challenging polymerases are able to exchange. The similarities in processivities between the gp4-ΔC17 experiments (5 ± 1 kb) and the 3.3 ± 0.6 kb observed here when WT polymerase and gp4 were chased with a high concentration of challenging Y526F (Fig. 4*B*), provide experimental support that an excess polymerase associated with the replisome gains access to the fork through stochastic dissociations of the synthesizing polymerase. Our current single-molecule experiments also provide additional support that exchange is mediated through interactions between the polymerase and gp4. To verify that it is indeed this interaction with the C-terminal tail of gp4 that permits exchange, we preassembled WT polymerase and gp4-ΔC17 and initiated DNA

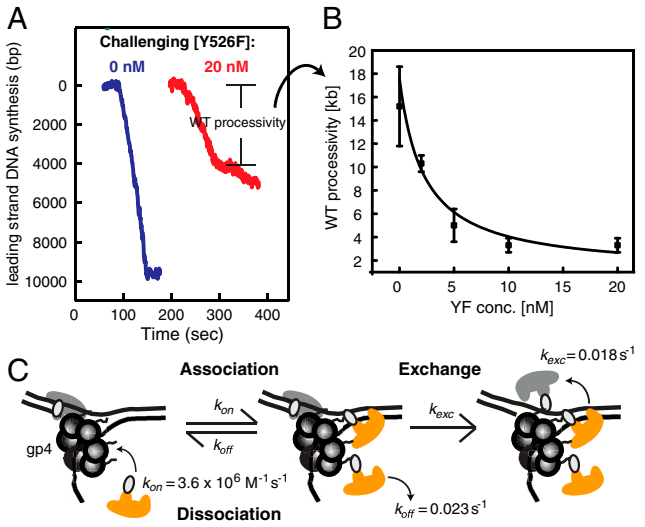

Fig. 4. The processivity of an individual DNA polymerase depends on the concentration of free polymerase in solution. (*A*) DNA synthesis trajectories of a preassembled WT leading-strand polymerase in the absence (*Left*) and presence (*Right*) of Y526F. (*B*) Titration curve depicting how the average processivity of the preassembled WT polymerase decreases as a function of challenging Y526F concentration. (*C*) Kinetic model describing polymerase exchange in the T7 replisome. Excess polymerases (orange) associate with the C-terminal tails of gp4 monomers. A transient dissociation of the synthesizing polymerase (gray) allows for exchange to occur.

synthesis in the presence of 20 nM challenging Y526F. As anticipated, the average WT processivity decreased to 5.8 ± 1.4 kb (*SI Text*). Importantly, the percentage of trajectories showing a change in DNA synthesis rate consistent with exchange decreased from 75% for WT gp4 to below 10% for gp4-ΔC17. This significant change in exchange efficiency shows that the C-terminal tail of gp4 plays a crucial role in recruiting and tethering polymerases from solution to the replisome.

Discussion

Our current single-molecule experiments indicate that polymerases are recruited to the fork through interactions with gp4, and that these interactions serve to increase the local polymerase concentration. Previous surface plasmon resonance experiments have found at least two binding modes between the T7 polymerase and the hexameric gp4 helicase/primase (16, 32). In the first, the "tight" binding mode, the polymerase is strongly associated with the primer template in a gp4-dependent manner with a half life on the DNA of greater than 10 min. The second or "loose" binding mode is much weaker and DNA-independent; it results from the electrostatic interaction of the acidic C-terminal tail of gp4 with the basic residues in the thioredoxin binding domain of gp5. Previous single-molecule studies concluded that this loose binding mode acts to confer processivity by retaining the polymerase at the fork when the enzyme transiently dissociates from the primer template due to disruption of the tight interaction. We show here that when challenged, excess polymerases from solution are capable of associating with a free C-terminal tail of one of the gp4 monomers and subsequently exchanging upon transient dissociation of the synthesizing polymerase (see Fig. 4*C*).

A powerful aspect of the single-molecule assay we describe is the ability to directly observe the association of soluble polymerases with the replication fork in the context of an actively synthesizing replisome. Fitting the Y526F titration data of Fig. 4*B* yields an apparent K_d of 11 nM for the interaction between polymerase and a single gp4 C-terminal tail. Given the measured k_{off} from the fluorescence experiments, we calculate a k_{on} of 3.6×10^6 M^{-1} sec^{-1}, a value consistent with the diffusion-limited bimolecular association rate constant that is consistent with the size of the T7 polymerase. At Y526F concentrations greater than the K_d, multiple polymerases occupy binding sites on the hexameric gp4. Given the values of k_{on} and k_{off}, we can calculate the average polymerase occupancy of gp4 for a given polymerase concentration, assuming each monomer of gp4 is an equivalent binding site. At a concentration of 20 nM polymerase, on average 4.8 of the 5 remaining binding sites on gp4 are occupied. With the binding sites of gp4 saturated, one can calculate the average time to exchange by dividing the average processivity at high concentrations of challenging Y526F (3.3 kb) by the average WT leading-strand synthesis rate (122 bp/s), yielding a value of τ_{exc} of 27 s, which is consistent with estimates from our fluorescence experiments. The on and off rates measured in our experiments suggest that the exchange mechanism we observe in vitro is operational in vivo. Estimates of the in vivo concentration of the T7 polymerase in an infected *E. coli* cell range from 150 nM to 1 μM, suggesting that gp4 is similarly saturated with polymerases under physiological conditions (33). This significant increase in polymerase concentration at the replication fork likely plays an important role in increasing replisome processivity along with promoting efficient loading of lagging-strand polymerases onto nascent Okazaki fragments.

The observed delay time between polymerase association and exchange has important implications for how the replisome might regulate access of various proteins to the replication fork. Studies involving the *E. coli* (13, 14) and bacteriophage T4 (11) replisomes have found that polymerase exchange is mediated through interactions between the polymerase and sliding clamp, similar to the interaction between polymerase and gp4 for the T7 replisome. We find that excess polymerase associated with gp4 has little to no effect on the propensity of the synthesizing polymerase to exchange. Instead, the loosely associated polymerase remains inactive until the synthesizing polymerase transiently dissociates from the primer. This is evident by comparing the nearly identical average processivities of the ΔC17 and Y526F chase experiments, excluding an allosteric exchange mechanism in which the loosely associated polymerase promotes displacement of the engaged polymerase. The dissociation of the T7 polymerase from the primer likely occurs during the translocation step in which the polymerase must move to the next templating base as the lifetime of the bound state for a synthesizing polymerase is dramatically less than for an idle one (16). Whether polymerase exchange in other prokaryotic systems results from the stochastic dissociation of the synthesizing polymerase, polymerase stalling (13), or regulatory mechanisms such as the SOS response (34) is still unclear. The single-molecule methods presented here represent a powerful and unique approach to explore these questions.

By combining the mechanical manipulation of DNA with the observation of individual fluorescent proteins, we have been able to simultaneously monitor the activity and composition of a complex molecular machine. The assay presented here should be broadly applicable to answer structure-function questions for multiprotein complexes acting on DNA. Future refinements of this assay, including improved spatial resolution and the incorporation of standard single-molecule fluorescence techniques (35) such as FRET and anisotropy will allow for greater structural insight and provide a means to directly connect conformational changes with the activity of a multiprotein complex.

Methods

Protein Purification. Previously published protocols were used to prepare T7 DNA polymerase (1:1 complex of gp5 and trx) (36), gp5 (36), trx (36), gp4 (37), gp4-ΔC17 (37), and Y526F polymerase (12).

Combined Single-Molecule Fluorescence and DNA Flow Stretching Measurements. A DNA construct based on λ phage DNA with replication fork and primer was tethered to the surface of functionalized coverslip through a biotin-streptavidin linker. The flow of buffer through the flow cell stretched the tethered DNA whereas antidigoxigenin coated quantum dots bound to

the DNA were used to visualize DNA length. Leading-strand synthesis reactions result in the shortening of the DNA construct due to the conversion of the lagging-strand into ssDNA, as monitored by tracking the motion of the quantum dots. The association of fluorescently labeled polymerases with the replisome was observed using single-molecule TIRF microscopy. A two-color imaging scheme allows for continuous observation of DNA synthesis activity while stroboscopically probing polymerase stoichiometry at the replication fork. For a full description, see *SI Text*.

ACKNOWLEDGMENTS. We thank Dr. Samir Hamdan for many helpful discussions and for providing the purified thioredoxin, gp5, and the gp4-ΔC17 used in this study. We also thank Dr. Masateru Takahashi for the gift of Y526F and Dr. Johannes Walter for a critical reading of the manuscript. This work was supported by a Jane Coffin Childs postdoctoral fellowship (to J.J.L), the National Institutes of Health Grants GM-077248 (A.M.v.O) and GM-54397 (C.C.R.), and the National Science Foundation CAREER Grant 0543784 (A.M.v.O.).

1. Langston LD, Indiani C, O'Donnell M (2009) Whither the replisome: Emerging perspectives on the dynamic nature of the DNA replication machinery. *Cell Cycle* 8:2686–2691.
2. Benkovic SJ, Valentine AM, Salinas F (2001) Replisome-mediated DNA replication. *Annu Rev Biochem* 70:181–208.
3. Pomerantz RT, O'Donnell M (2008) The replisome uses mRNA as a primer after colliding with RNA polymerase. *Nature* 456:762–766.
4. Wang TC (2005) Discontinuous or semi-discontinuous DNA replication in *Escherichia coli*. *Bioessays* 27:633–636.
5. Lopes M, Foiani M, Sogo JM (2006) Multiple mechanisms control chromosome intregrity after replication fork uncoupling and restart at irreparable UV lesions. *Mol Cell* 21:15–27.
6. Heller RC, Marians KJ (2006) Replication fork reactivation downstream of a blocked nascent leading strand. *Nature* 439:557–562.
7. Alberts BM, et al. (1983) Studies on DNA replication in the bacteriophage T4 in vitro system. *Cold Spring Harb Sym* 47:655–668.
8. Debyser Z, Tabor S, Richardson CC (1994) Coordination of leading and lagging strand DNA synthesis at the replication fork of bacteriophage T7. *Cell* 77:157–166.
9. Kadyrov FA, Drake JW (2001) Conditional coupling of leading-strand and lagging strand DNA synthesis at bacteriophage T4 replication forks. *J Biol Chem* 276:29559–29566.
10. Kim S, Dallmann HG, McHenry CS, Marians KJ (1996) τ couples the leading- and lagging-strand polymerases at the *Escherichia coli* DNA replication fork. *J Biol Chem* 271:21406–21412.
11. Yang J, Zhuang Z, Roccasecca RM, Trakselis MA, Benkovic SJ (2004) The dynamic processivity of the T4 DNA polymerase during replication. *Proc Natl Acad Sci USA* 101:8289–8294.
12. Johnson DE, Takahashi M, Hamdan SM, Lee S-J, Richardson CC (2007) Exchange of DNA polymerases at the replication fork of bacteriophage T7. *Proc Natl Acad Sci USA* 104:5312–5317.
13. Indiani C, McInerney P, Georgescu R, Goodman MF, O'Donnell M (2005) A sliding-clamp toolbelt binds high- and low-fidelity DNA polymerases simultaneously. *Mol Cell* 19:805–815.
14. Indiani C, Langston LD, Yurieva O, Goodman MF, O'Donnell M (2009) Translesion DNA polymerases remodel the replisome and alter the speed of the replicative helicase. *Proc Natl Acad Sci USA* 106:6031–6038.
15. Hamdan SM, Richardson CC (2009) Motors, switchesm and contacts in the replisome. *Annu Rev Biochem* 78:205–243.
16. Hamdan SM, et al. (2007) Dynamic DNA helicase-DNA polymerase interactions assure processive replication fork movement. *Mol Cell* 27:539–549.
17. van Mameren J, Peterman EJ, Wuite GJ (2008) See me, feel me: Methods to concurrently visualize and manipulate single DNA molecules and associated proteins. *Nucleic Acids Res* 36:4381–4389.
18. Lang MJ, Fordyce PM, Engh AM, Neuman KC, Block SM (2004) Simultaneous, coincident optical trapping and single-molecule fluorescence. *Nat Methods* 1:133–139.
19. Hohng S, et al. (2007) Fluorescence-force spectroscopy maps two-dimensional reaction landscape of the Holliday junction. *Science* 318:279–283.
20. van Mameren J, et al. (2009) Counting Rad51 proteins disassembling from nucleoprotein filaments under tension. *Nature* 457:745–748.
21. Lee J-B, et al. (2006) DNA primase acts as a molecular brake during DNA replication. *Nature* 439:621–624.
22. Tanner NA, et al. (2008) Single-molecule studies of fork dynamics in *Escherichia coli* DNA replication. *Nat Struct Mol Biol* 15:170–176.
23. Strick T, Allemand JF, Croquette V, Bensimon D (2000) Twisting and stretching single DNA molecules. *Prog Biophys Mol Bio* 74:115–140.
24. Bustamante C, Bryant Z, Smith SB (2003) Ten years of tension: single-molecule DNA mechanics. *Nature* 421(Suppl 6921):423–427.
25. Wuite GJL, Smith SB, Young M, Keller D, Bustamante C (2000) Single-molecule studies of the effect of template tension on T7 DNA polymerase activity. *Nature* 404:103–106.
26. Maier B, Bensimon D, Croquette V (2000) Replication by a single DNA polymerase of a stretched single-stranded DNA. *Proc Natl Acad Sci USA* 97:12002–12007.
27. Axelrod D (1989) Total internal reflection fluorescence microscopy. *Methods Cell Biol* 30:245–270.
28. Kuhn H, Frank-Kamenetskii MD (2008) Labeling of unique sequences in double-stranded DNA at sites of vicinal nicks generated by nicking endonucleases. *Nucleic Acids Res* 36:e40.
29. Kochaniak AB, et al. (2009) Proliferating cell nuclear antigen uses two distinct modes to move along DNA. *J Biol Chem* 284:17700–17710.
30. Etson CM, Hamdan SM, Richardson CC, van Oijen AM (2010) Thioredoxin suppresses microscopic hopping of T7 DNA polymerase on duplex DNA. *Proc Natl Acad Sci USA* 107:1900–1905.
31. Tabor S, Richardson CC (1995) A single residue in DNA polymerases of the *Escherichia coli* DNA polymerase I family is critical for distinguishing between deoxy- and dideoxyribonucleotides. *Proc Natl Acad Sci USA* 92:6339–6343.
32. Hamdan SM, et al. (2005) A unique loop in T7 DNA polymerase mediates the binding of helicase-primase, DNA binding protein, and processivity factor. *Proc Natl Acad Sci USA* 102:5096–5101.
33. Richardson CC (1983) Replication of bacteriophage T7 DNA. *Developments in Molecular Virology,* ed Y Becker pp:93–100.
34. Opperman T, Murli S, Smith BT, Walker GC (1999) A model for a umuDC-dependent prokaryotic DNA damage checkpoint. *Proc Natl Acad Sci USA* 96:9218–9223.
35. Joo C, Balci H, Ishitsuka Y, Buranachai C, Ha T (2008) Advances in single-molecule fluorescence methods for molecular biology. *Annu Rev Biochem* 77:51–76.
36. Tabor S, Huber HE, Richardson CC (1987) *Escherichia coli* thioredoxin confers processivity on the DNA polymerase activity of the gene 5 protein of bacteriophage T7. *J Biol Chem* 262:16212–16223.
37. Notarnicola SM, Mulcahy HL, Lee J, Richardson CC (1997) The acidic carboxyl terminus of the bacteriophage T7 gene 4 helicase/primase interacts with T7 DNA polymerase. *J Biol Chem* 272:18425–18433.